Combining Microwave Radiometer and Wind Profiler Radar Measurements for High-Resolution Atmospheric Humidity Profiling

Laura Bianco and Domenico Cimini

Centre of Excellence CETEMPS, University of L'Aquila, Coppito, Italy, and Cooperative Institute for Research in Environmental Science, NOAA/Environmental Technology Laboratory, University of Colorado, Boulder, Colorado

Frank S. Marzano

Centre of Excellence CETEMPS, University of L'Aquila, Coppito, Italy

Randolph Ware

Radiometrics Corporation, and University Corporation for Atmospheric Research, Boulder, Colorado

ABSTRACT

A self-consistent remote sensing physical method to retrieve atmospheric humidity high-resolution profiles by synergetic use of a microwave radiometer profiler (MWRP) and wind profiler radar (WPR) is illustrated. The proposed technique is based on the processing of WPR data for estimating the potential refractivity gradient profiles and their optimal combination with MWRP estimates of potential temperature profiles in order to fully retrieve humidity gradient profiles. The combined algorithm makes use of recent developments in WPR signal processing, computing the zeroth-, first-, and second-order moments of WPR Doppler spectra via a fuzzy logic method, which provides quality control of radar data in the spectral domain. On the other hand, the application of neural network to brightness temperatures, measured by a multichannel MWRP, can provide continuous estimates of tropospheric temperature and humidity profiles. Performance of the combined algorithm in retrieving humidity profiles is compared with simultaneous in situ radiosonde observations (raob's). The empirical sets of WPR and MWRP data were collected at the Atmospheric Radiation Measurement (ARM) Program's Southern Great Plains (SGP) site. Combined microwave radiometer and wind profiler measurements show encouraging results and significantly improve the spatial vertical resolution of atmospheric humidity profiles. Finally, some of the limitations found in the use of this technique and possible future improvements are also discussed.

1. Introduction

Monitoring of humidity profiles in the lower troposphere has been one of the main goals of recent meteorological research due to its importance for atmospheric dynamics and microphysics. To this aim both passive and active remote sensing techniques have been proposed and successfully applied (Gossard et al. 1982; Stankov et al. 1996; Solheim et al. 1998; MacDonald et al. 2002; Stankov et al. 2003; Ware et al. 2003).

A major focus of current remote sensing research is

Corresponding author address: Dr. Laura Bianco, CETEMPS, Universita' degli Studi de L'Aquila, Dip. Fisica dell'Atmosfera, via Vetoio, 67010, Coppito, L'Aquila, Italy.
E-mail: Laura.Bianco@aquila.infn.it

to evaluate the capability of these instruments to remotely derive meteorological quantities using sensor synergy (Stankov 1998). An appealing application of this concept to the retrieval of high-resolution atmospheric humidity profiles is the synergetic use of ground-based instruments only, such as either a combination of radar wind profilers and Global Position System (GPS) receivers or either a combination of radar wind profilers and microwave radiometers (Stankov et al. 1996; Gossard et al. 1999; Furumoto et al. 2003; Bianco et al. 2003). In particular, the last approach has significant potential due to the profiling capability of both sensors and the possibility to estimate the atmospheric state in terms of wind, humidity, temperature, and cloud liquid.

For what concerns the wind profiler radar (WPR),

atmospheric boundary layer parameters currently obtained by Doppler remote sensing system are derived from the first three moments of the measured Doppler spectra (Gossard et al. 1982, 1998). However, radar signals at most sites often show contamination from other sources, such as ground clutter, intermittent clutter, radio frequency interference, and sea clutter. For the wind, signal-processing techniques have been developed to isolate the true atmospheric signal from the measured spectra (May and Strauch 1989; Wilczak et al. 1995; Cornman et al. 1998; Jordan et al. 1997). To obtain accurate moments for the desired atmospheric spectral peak, in addition to using a physically based algorithm (Weber et al. 2004), it is worth using and testing an algorithm that makes use of recent developments in wind profiler radar signal processing, computing the zeroth, first, and second moments of wind profiler radar Doppler spectra via a fuzzy logic method (Bianco and Wilczak 2002), which provides quality control of radar data in the spectral domain. To retrieve high-resolution humidity profiles in a combined sensor approach, the zeroth, first, and second moments, computed by the fuzzy logic algorithm, can be employed to compute the structure parameter of potential refractivity (C_ϕ^2), the horizontal wind (V_h), and the structure parameter of vertical velocity (C_w^2), respectively (Stankov et al. 2003). The quantities C_ϕ^2, V_h, and C_w^2 can then be properly used together to retrieve the potential refractivity gradient profiles ($d\phi/dz$).

Microwave radiometer profiler (MWRP) can provide accurate tropospheric water vapor and temperature profiles when operating in the 20–60 GHz (Westwater 1993; Solheim and Godwin 1998). Both statistical and neural network approaches can be used to retrieve atmospheric profiles by generating synthetic datasets of brightness temperature from radiosonde profile archives processed with radiative transfer models (Schroeder and Westwater 1991; Güldner and Spänkuch 2001; Solheim et al. 1998). Significant improvements in radiometric retrieval accuracy and resolution using elevation scanning or adjustments in forward modeling have been reported (Liljegren 2004). However, the calibration of MWRP is an issue to be carefully considered (Han and Westwater 2000; Cimini et al. 2003). In a combined sensor perspective, microwave radiometer data can be used to estimate the potential temperature gradient profiles ($d\theta/dz$).

As a final step of a combined retrieval technique, profiles of $d\phi/dz$ derived from WPR, and $d\theta/dz$ derived from MWRP are sufficient to fully estimate humidity gradient profiles, as suggested by Stankov et al. (1996). The advantage of such a synergetic humidity retrieval technique is to increase the vertical resolution

of ground-based microwave radiometers, without loosing the high accuracy they can provide for integrated values, and to be completely independent from simultaneous radiosonde observations. Simultaneous in situ measurements by radiosonde can be used just as a comparison to check the improvements brought by the combined algorithm in retrieving humidity profiles.

The aim of this work is to set up and to investigate the potential of a combined retrieval algorithm exploiting WPR and MWRP measurements, following the approach described above. Section 2 introduces the instruments involved in this work, the characteristics of the experimental site, and the data analysis applied on the collected measurements. Section 3 gives the basic principles of the theory used for the retrieval of vertical humidity profiles with the combined use of $d\phi/dz$, obtained by radar wind profilers, and $d\theta/dz$, estimated from multichannel microwave radiometers. Section 4 presents results obtained for selected case studies, and discusses the limitations, which could be found in the application of such a technique. Finally, section 5 provides a summary of the results, discussing possible developments for future research.

2. Site, instruments, and data processing

The empirical sets of WPR and MWRP data were collected at the Atmospheric Radiation Measurement (ARM) Program's Southern Great Plains (SGP) site in Oklahoma (latitude: 36°37′N, longitude: 97°30′W, altitude: 313 m ASL). In this work we have focused on few case studies: in particular, we considered days 1, 3, 6, 7, and 17 June 2002. Some quantitative results are provided, although an extensive analysis, concerning an extended dataset, is also in preparation and will be a topic of future works.

a. Wind profiler radar

The wind profiler radar is a 915-MHz five-beam radar manufactured by Radian Corporation. It operates by transmitting electromagnetic energy into the atmosphere and measuring the strength and frequency of backscattered energy. It consists of a single-phased microstrip antenna array consisting of nine "panels." The antenna is approximately 4 m square and is oriented in a horizontal plane so the "in-phase" beam travels vertically. Radial components of motion along each pointing direction are determined sequentially. It takes, nominally, 30–45 s (dwell time) to determine the radial components from a single pointing direction. Thus, the system cycles through five beams (south, north, east, west, and vertical) at low power, and then cycles the

five beams again at a high power (longer pulse length) setting. Then the whole process is repeated. About 5 min elapse before the system returns to the beginning of its sequence. Within an averaging interval, the estimates from each beam-power combination are saved and these values are examined and compared at the end of the period to determine the consensus-averaged radial components of motion. The model used in this work is the high resolution/low maximum height that sampled the boundary layer from 90- to 2500-m height in the vertical at a 60-m resolution.

THE FUZZY LOGIC RETRIEVAL METHOD

The correct computation of the first three moments of the Doppler spectra from radar wind profiling data is crucial for the use of these instruments to derive parameters other than winds. The mean velocity profile, obtained from the first moment of the Doppler spectrum, was one of the earliest quantities extracted from remote sensing observations. On the other hand, the second moment of the Doppler spectrum (when the radars are pointing vertically) has not been widely exploited, and its use is still in the research and evaluation stage. It is a measure of the broadening of the Doppler spectrum due to a variety of factors, including velocity variance resulting from atmospheric turbulence on scales smaller than the pulse volume. It has the potential to provide profiles of turbulence quantities, such as eddy dissipation rate and structure parameters, continuously in time.

Over the last two decades several attempts have been made to use spectral width from profilers to measure the turbulence intensity without much success (Gossard et al. 1990; Cohn 1995). This suggests the degree of difficulty of the measurement. The principal problem is related to the fact that contamination by unwanted targets is especially detrimental to second-moment calculations and that other nonturbulent processes also contribute to the broadening. To be able to use the spectral width to measure turbulence intensities, it is necessary to be certain that the entire scatter is due to turbulence. For all these reasons it was found that a new treatment of the radar data was necessary.

Here, we use fuzzy logic to compute the first three moments of the radar Doppler spectrum and the procedure we use is outlined below. Additional details on the implementation of the method, including the mathematical formulations of the membership functions and the rules for applying them, can be found in Bianco and Wilczak (2002). Fuzzy logic algorithms can be very useful for atmospheric spectral peak recognition, where the data are often contaminated by the presence of nonatmospheric clutter signals. Following the initial idea of Cornman et al. (1998), we determine the characteristics of different kinds of clutter and atmospheric peaks in real situations and develop an algorithm to differentiate among them.

The construction of the fuzzy logic algorithm begins with a two-dimensional matrix of observations, with dimensions representing the number of range gates and the number of spectral frequency (or velocity) points. For each matrix point several parameters are computed. These parameters are "power density ratio" (ratio of the amplitude of the spectrum at each frequency to a background average minimum spectral level associated with system noise), "gradient" and "curvature" (characterizing the slope of the spectrum along the radial velocity axis), "asymmetry" (defined at each frequency point f, as the absolute value of the difference between the value of the spectrum at $+f$ and $-f$), "radial velocity values" (used to differentiate the clutter from stationary targets, which will always have small radial velocities, from atmospheric peaks that will typically have larger radial velocities), and "skewness" (defined as the degree of asymmetry of the entire spectrum around zero velocity). Each parameter may be used to determine if a matrix point belongs to a spectral peak, if the point contains clutter, or both. These parameters are used as input for the fuzzy logic algorithm for the spectral peak identification. They are combined together with the use of membership functions and rules. We note that the characteristics of both the membership functions and the sets of rules are based on the principal differences between atmospheric and clutter signals. The skill of the fuzzy logic's algorithms depends on the correct identification of the membership functions to adopt, and on constructing an appropriate set of rules.

At the end of the fuzzy logic procedures we have an output, which is a total score field (i.e., a matrix with dimensions the same as the starting spectral matrix) that gives each spectral point a score. Negative values indicate that the point is influenced by clutter; positive values indicate that it has an atmospheric signal, and near-zero values indicate that the point is part of the noise floor of the spectrum. At each spectral point where the score is negative, the spectral value is replaced by a random noise value determined from the noise characteristics of the original spectrum. The resulting spectrum is then used for the moment's estimation.

As an example, in Fig. 1 we show the time–height cross section of range corrected signal-to-noise ratio (SNR) obtained by the 915-MHz radar for one of the days under observation (1 June 2002). On that day our postprocessing fuzzy logic algorithm outperforms the
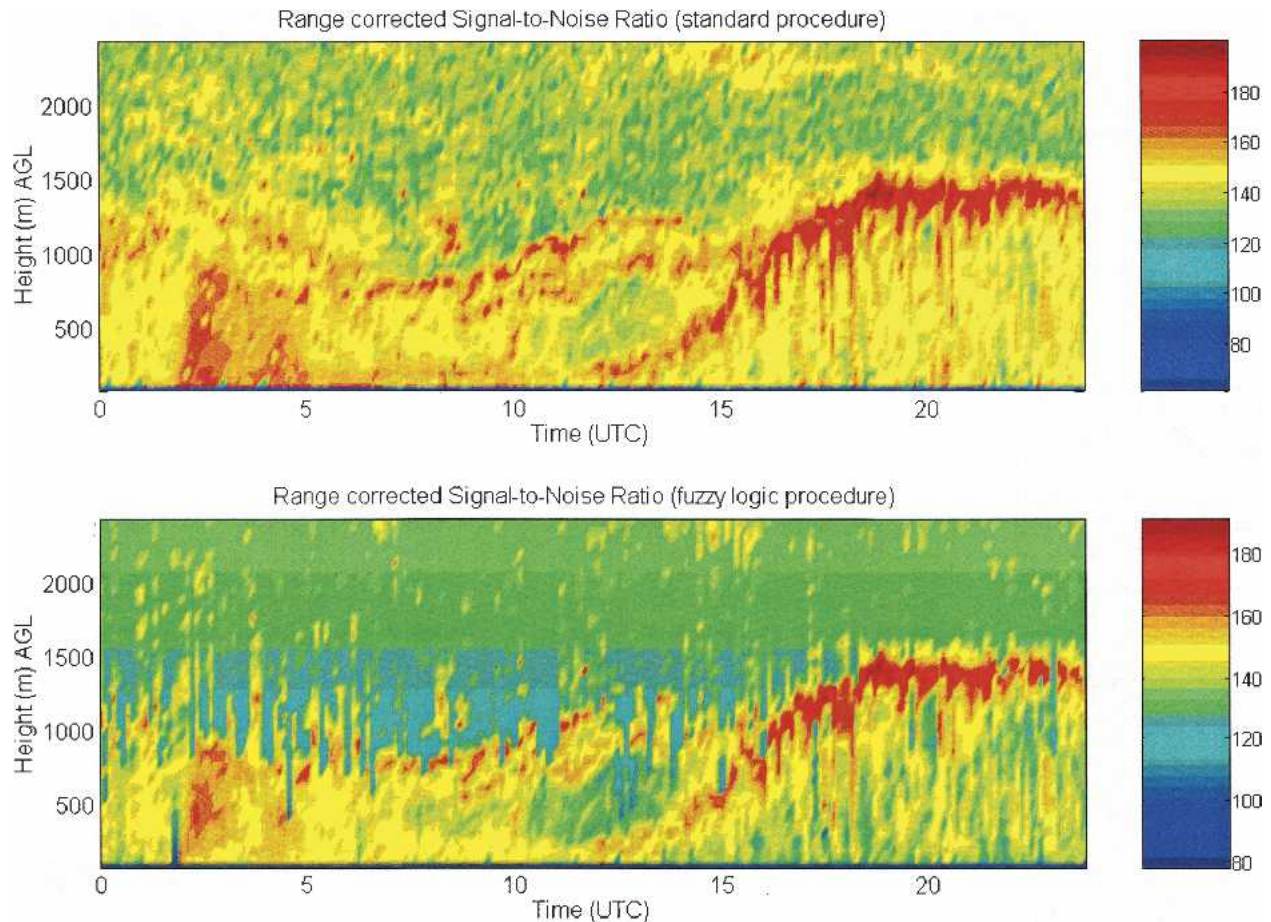
FIG. 1. (top) Time–height cross section of range-corrected SNR obtained for 1 Jun 2002 at the ARM SGP site by (top) the standard procedure (Strauch et al. 1984) and (bottom) fuzzy logic.

standard procedure, which uses the method of Strauch et al. (1984) by clearly reducing the noise above the boundary layer. Hereafter time is UTC (local daylight time = UTC − 5 h).

For the 915-MHz radar wind profiler data used in the present analysis, no fewer than eight individual spectral acquisitions are taken of the vertical beam each hour. Hourly profiles of the potential refractivity gradient ($d\phi/dz$) are determined by calculating the hourly median profiles of C_ϕ^2 and C_w^2 obtained by the fuzzy logic spectral peak identification procedure. The postprocessing procedure makes use of the raw spectral data.

Hourly vertical profiles are computed for the hour past the raob launch. The fuzzy logic postprocessing algorithm incorporates information from the vertical profiles of the variance of SNR over the chosen time period and the variance of vertical velocity measured by the vertical beam of the wind profiler over the same time period (Bianco and Wilczak 2002). In this perspective the time period of one hour was chosen so that the temporal variances are calculated at each range gate from the eight or more subhourly acquisitions.

Vertical profiles of the gradient of the horizontal wind (V_h) are, at a first step, computed using the horizontal components of the wind saved by the profiler in the consensus files. Briefly, consensus averaging consists of determining if a certain percentage (50%) of the values falls within a certain range of each other (2 m s^{-1} for the vertical beam, 3 m s^{-1} for oblique beams). If they do, those values are averaged to produce the radial wind estimate. The radial values are then combined to produce the wind profile. The results of this averaging process are what are reported in the consensus data files produced by the ARM data system. Included in these files are height, speed, direction, radial components, number of values in consensus, and SNR.

For the retrieval of the humidity gradient profiles, we first used consensus files as provided by ARM, without additional postprocessing performed on the spectra data. However, in a later step of our analysis, moments

obtained by the postprocessing procedure have been used to recompute horizontal winds.

b. Microwave radiometer profiler

The multichannel microwave profiler is a frequency-synthesized radiometer (Solheim and Godwin 1998), manufactured by Radiometrics (TP/WVP-3000). It observes atmospheric brightness temperature (Tb) at 12 frequencies in a region of the microwave spectrum that is dominated by emission of atmospheric water vapor, cloud liquid water, and molecular oxygen. By observing radiated power at selected frequencies in this region, the integrated water vapor (IWV), the cloud liquid water path (LWP), and the profile of temperature and humidity can be estimated (Ware et al. 2003). Observation frequencies (22.035, 22.235, 23.835, 26.235, 30.00, 51.25, 52.28, 53.85, 54.94, 56.66, 57.29, 58.80 GHz) were chosen through eigenvalue analysis to optimize profile retrieval accuracy (Solheim et al. 1998).

The radiometer is composed of two separate subsystems in the same cabinet, one for temperature (50–60 GHz) and the other for water vapor (20–30 GHz) profiling that share the same antenna and antenna pointing system. The system includes also surface meteorological sensors measuring air temperature, barometric pressure, and relative humidity, and a vertically pointing infrared thermometer providing cloud base information.

The radiometer output is continuously calibrated with a highly stable noise diode and an internal ambient target used as references, although tipping curves and cryogenic load tests are also often performed (Han and Westwater 2000; Cimini et al. 2003).

Neural network–based retrieval

Solheim et al. (1998) found through analysis on synthetic datasets that artificial neural network outperforms other inversion methods for retrieving water vapor, cloud liquid water, and temperature profiles from radiometric data. Therefore, the MWRP operational software was developed with the Stuttgart Neural Network Simulator, using a standard back-propagation algorithm for training, and a standard feed-forward network for profile determination. A set of historical radiosondes, launched at the ARM SGP site, has been processed with a radiative transfer model (Schroeder and Westwater 1991) in order to build up a training database for the neural network, based on microwave, infrared, and surface meteorological observations. Although the number of independent measurements (number of radiometric and meteorological measurements) is significantly less than the number of retrieved

layers (Güldner and Spänkuch 2001), profiles are output in 100-m increments altitudes up to 1 km and at 250-m increments from 1 to 10 km. Above about 7 km the atmospheric water vapor density and temperature approach a climatological mean value.

For one of the days under observation (1 June 2002), the time–height cross section of temperature T (K), absolute humidity ρ (g m^{-3}), retrieved by the MWRP, are presented in Fig. 2. We also show the time–height cross section of potential temperature θ (K) as derived from the MWRP observations. We show only the first 2500 m in order to match the WPR vertical range and thus compare with Fig. 1. The temperature shows a clear diurnal variation, with the development of an inversion layer during the night hours up to the 1300 UTC when the convection starts to grow. As a consequence the water vapor scale height increases and the potential temperature transits from stratified conditions to a well-developed mixing within the convective boundary layer.

3. Combined approach basis

The theory used for the retrieval of humidity profiles from wind profiler observations is well explained in Stankov et al. (2003) and will be briefly recalled here. Following Gossard et al. (1995), we define potential refractivity ϕ as

$$\phi = \frac{77.6 p_r}{\theta}\left(1 + \frac{7.73 Q}{\theta}\right), \qquad (1)$$

where Q is the specific humidity (g kg^{-1}), $\theta = T(p_r/p)^{0.286}$ is the potential temperature (K), and p_r is the reference pressure (mb).

The linearized equation for small perturbations is (Gossard et al. 1995)

$$d\phi = \frac{\partial \phi}{\partial \theta} d\theta + \frac{\partial \phi}{\partial Q} dQ, \qquad (2)$$

where

$$\frac{\partial \phi}{\partial \theta} = -\frac{77.6 p_r}{\theta^2}\left(1 + 15.46 \frac{Q}{\theta}\right) \equiv -a_0,$$

$$\frac{\partial \phi}{\partial Q} = 77.6 p_r\left(\frac{7.73}{\theta^2}\right) \equiv b_0. \qquad (3)$$

In this work a_0 and b_0 are computed from vertical profiles of Q and θ as respectively measured and retrieved by the MWRP. Their values are found to be constant, as already predicted by Gossard et al. (1982) within the vertical range of interest, and particularly $a_0 \approx 1$ and $b_0 \approx 6$, for this dataset.
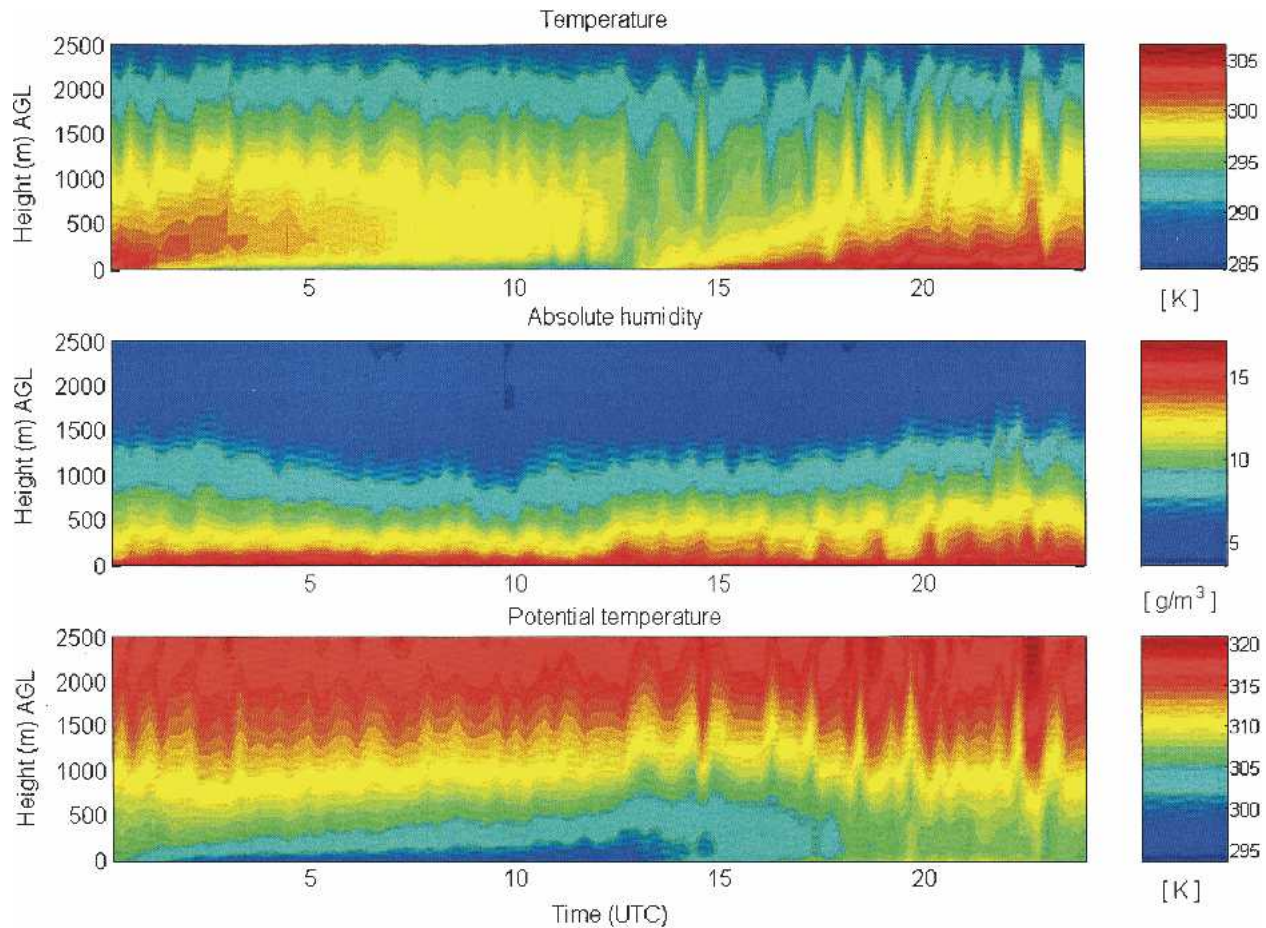
FIG. 2. Time–height cross section of (top) temperature T, (middle) absolute humidity ρ, and (bottom) potential temperature θ. Profile of θ is estimated from profiles of T and P, which are retrieved from MWRP measurements for 1 Jun 2002 at the ARM SGP site.

From Eq. (2),

$$\frac{dQ}{dz} = (b_0)^{-1}\left(\frac{d\phi}{dz} + a_0\frac{d\theta}{dz}\right)(\text{g kg}^{-1}\text{ m}^{-1}). \qquad (4)$$

This gives the vertical profile of humidity gradient as a function of vertical profiles of potential refractivity and potential temperature gradients. By integrating the vertical profile of dQ/dz, we can therefore compute the vertical profile of Q. In our approach we constrain the value of Q at the first level of the profile, which is the first available measurement obtained by the wind profiler, to be equal to the MWRP retrieval at the same level. Moreover, the humidity profile is scaled in order to match the MWRP water vapor content, integrated up to the maximum height reached by the WPR measurement. This is an important step because it guarantees that the original MWRP accuracy for integrated water vapor content is preserved in the product of the combined technique. We follow the approach used by ARM to scale radiosonde measurements by dual-

channel microwave radiometer observations (Turner et al. 2003; Westwater et al. 2003): the absolute humidity profile is scaled by a factor such that the integral up to the top boundary matches the integrated value estimated by the MWRP:

$$\rho_{\text{WPR+MWRP}} = K\,\rho_{\text{WPR}} = \frac{\displaystyle\int_{P_{\text{sur}}}^{P_{\text{top}}} \rho_{\text{MWRP}}\,dp}{\displaystyle\int_{P_{\text{sur}}}^{P_{\text{top}}} \rho_{\text{WPR}}\,dp}\,\rho_{\text{WPR}}.$$

$$(5)$$

Considering the given definition of the potential temperature, θ, we can estimate this quantity and its vertical gradient by using the temperature profile as retrieved by the MWRP together with the measurements of surface pressure and a prediction of the atmospheric scale height. Thus, we use the temperature profile retrieved by MWRP and the pressure reading from the
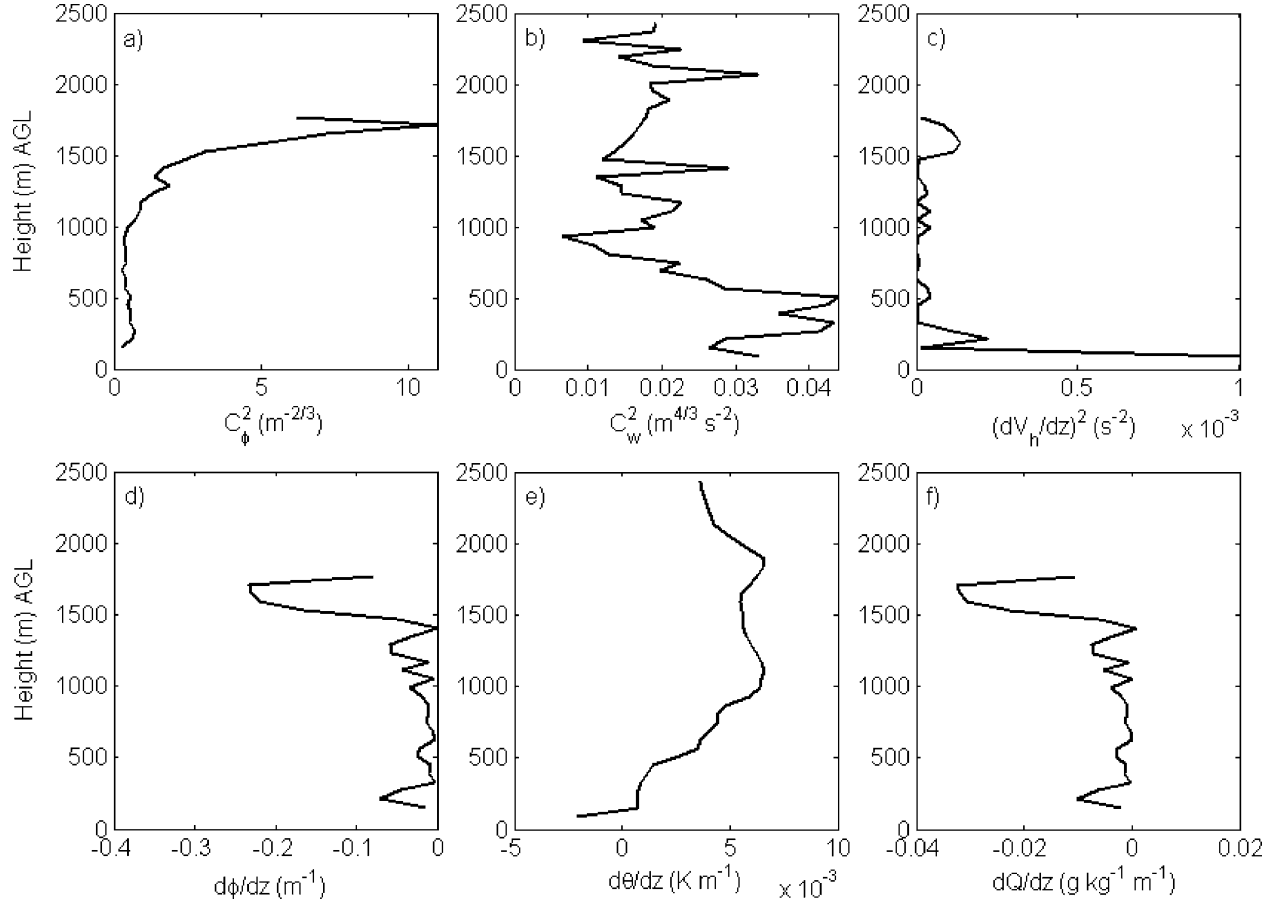
FIG. 3. 2330 UTC 7 Jun 2002: hourly radar-obtained vertical profiles for (a) C_ϕ^2, (b) C_w^2, (c) $(dV_h/dz)^2$, (d) $d\phi/dz$, (e) $d\theta/dz$ obtained from microwave radiometer measurements, and (f) retrieved humidity gradient profiles (dQ/dz) obtained from the combination of $d\phi/dz$ and $d\theta/dz$ with the use of Eq. (4).

MWRP surface sensor. Both error propagation analysis and a statistics over the set of collocated radiosonde and MWRP measurements indicate accuracy better than 5% for estimate of potential temperature profile up to 2 km.

Gossard et al. (1982, 1998) found that for homogeneous isotropic turbulence in a horizontally homogeneous medium with vertical gradients of mean properties, the vertical gradient of potential refractivity is

$$\left(\frac{d\phi}{dz}\right)^2 \approx \left(\frac{L_w}{L_\phi}\right)^{4/3}\left(\frac{dV_h}{dz}\right)^2\left(\frac{C_\phi}{C_w}\right)^2, \qquad (6)$$

where V_h is the horizontal wind (m s^{-1}), C_ϕ^2 is the structure parameter of potential refractivity (m$^{-2/3}$), and C_w^2 is the structure parameter of vertical velocity (m$^{4/3}$ s^{-2}). Calling ε the turbulent dissipation rate, then $C_w^2 = B_w\varepsilon^{2/3}$, where $B_w = 4/3\,B$, and $B = 2.1$ is the Kolmogorov constant; L_w and L_ϕ are the outer length scales for potential refractive index and shear defined in Gossard

et al. (1982). Note that in Eq. (6) we have the squared vertical gradient of potential refractivity, which therefore cannot be resolved unambiguously. Stankov et al. (2003) determined the sign of the radar-obtained $d\phi/dz$ by using radiosonde observations. In our approach we are able to compute the same quantity from Eq. (1) using microwave radiometer estimated profiles of Q and T, leaving our retrieval of vertical humidity profiles being completely independent from radiosonde measurements. Radar obtained values of $d\phi/dz$ are derived combining V_h, C_ϕ^2, and C_w^2, which are respectively related to the first, zeroth, and second moments' calculation of the radar-derived spectra acquisitions.

Here, V_h is obviously related to the estimation of the first moment (Doppler shift) in the spectral data. Vertical profiles of its gradient are, as a first step, computed using values of horizontal components collected in the consensus files by the wind profiler; as a second step they are recomputed on the moments obtained by the postprocessing procedure, and then used in Eq. (6).
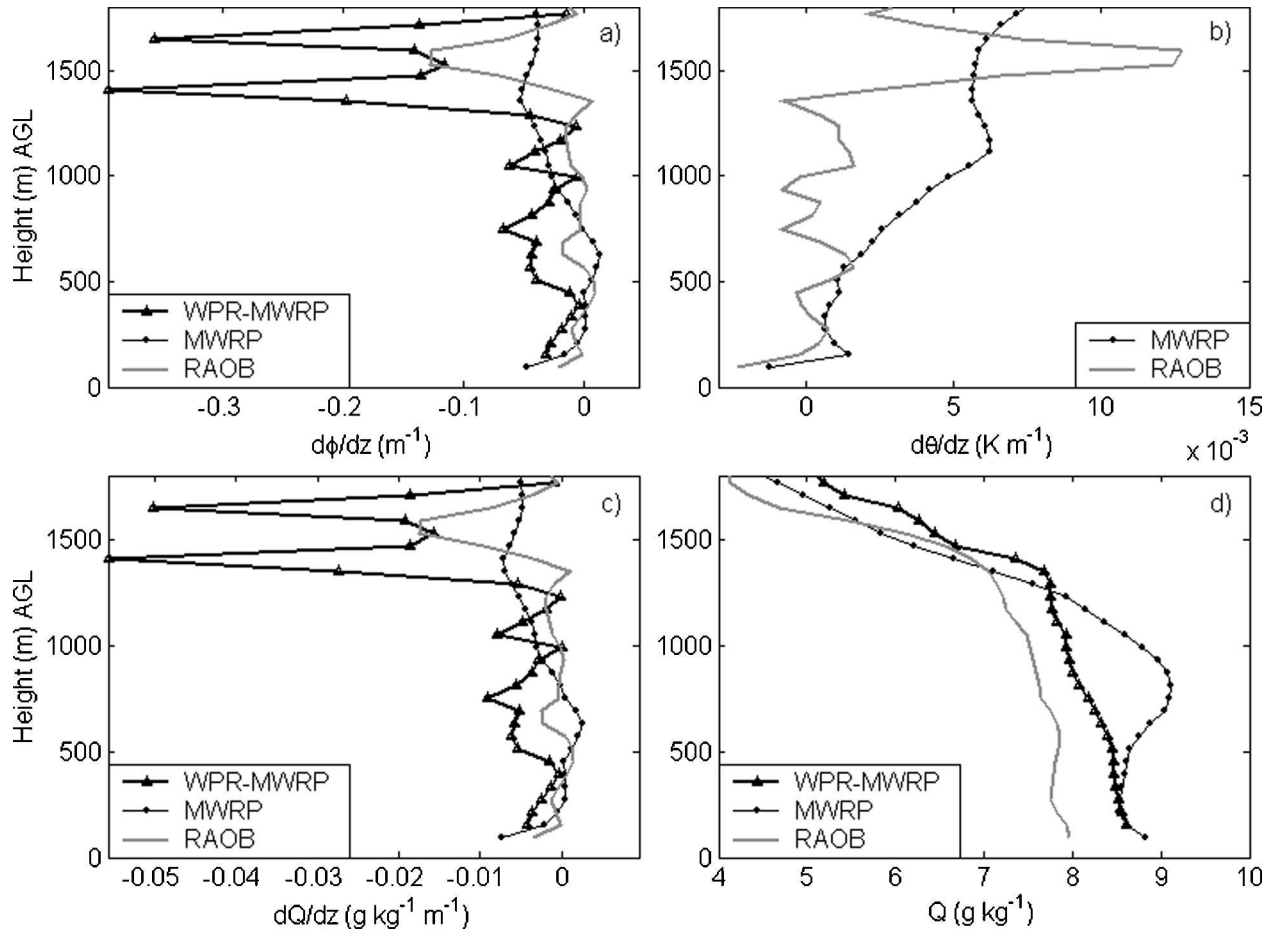
FIG. 4. 2330 UTC 6 Jun 2002: (a) hourly vertical profiles for $d\phi/dz$ as measured by radiosonde (solid gray line), estimated by MWRP (dotted line), and computed with the use of Eq. (6) (solid black line with triangles at measurement heights); (b) $d\theta/dz$ as measured by radiosonde (solid gray line) and estimated by MWRP (dotted line); (c) hourly vertical profiles for dQ/dz as measured by radiosonde (solid gray line), estimated by MWRP (dotted line), and computed with the combined technique (solid black line with triangles at measurement heights); (d) retrieved humidity vertical profiles (Q) obtained from the integration of dQ/dz in (c).

Here C_ϕ^2 is related to the structure parameter of refractive index C_n^2 (Gossard et al. 1982) through the relation

$$C_\phi^2 = e^{1.428z/H} C_N^2, \qquad (7)$$

where H is the scale height, $C_N^2 = C_n^2 \times 10^{12}$ from definition, and $N = (n - 1) \times 10^6$ (known as *radio refractivity*). Therefore, C_ϕ^2 is related to the estimation of the zeroth moments of the spectral data in accordance with (Stankov et al. 2003)

$$C_n^2 = \frac{1.54 \times 10^{-13} T_0}{\alpha^2 P_t n_c A_p} \lambda^{1/3} \left(\frac{R}{\Delta R} \right)^2 \Sigma. \qquad (8)$$

In this equation T_0 (system noise temperature), α^2 (which accounts for the losses in the transmission line), P_t (transmitted power), n_c (the number of coherent in-

tegrations), A_p (physical antenna area), λ (radar wavelength), R (range to the target), ΔR (range resolution) are all known, and Σ is the SNR estimated from the spectral data.

Here C_w^2 is related to the second moment of the radar-obtained spectra when only the vertical beam is working; C_w^2 is in fact related to the turbulent dissipation rate ε, which is in turn determined through the correct estimation of the broadening of the spectrum. According to Gossard (1990; see also Gossard et al. 1998), the broadening of the spectrum is first corrected to contributions due to the shear and to the antenna properties—second, it is necessary to account for the spatial and temporal filtering effects on the Doppler spectrum (White et al. 1999; Gossard et al. 1998).

Figure 3 shows a summary of the variables used in the retrieval of humidity gradient profiles and the result
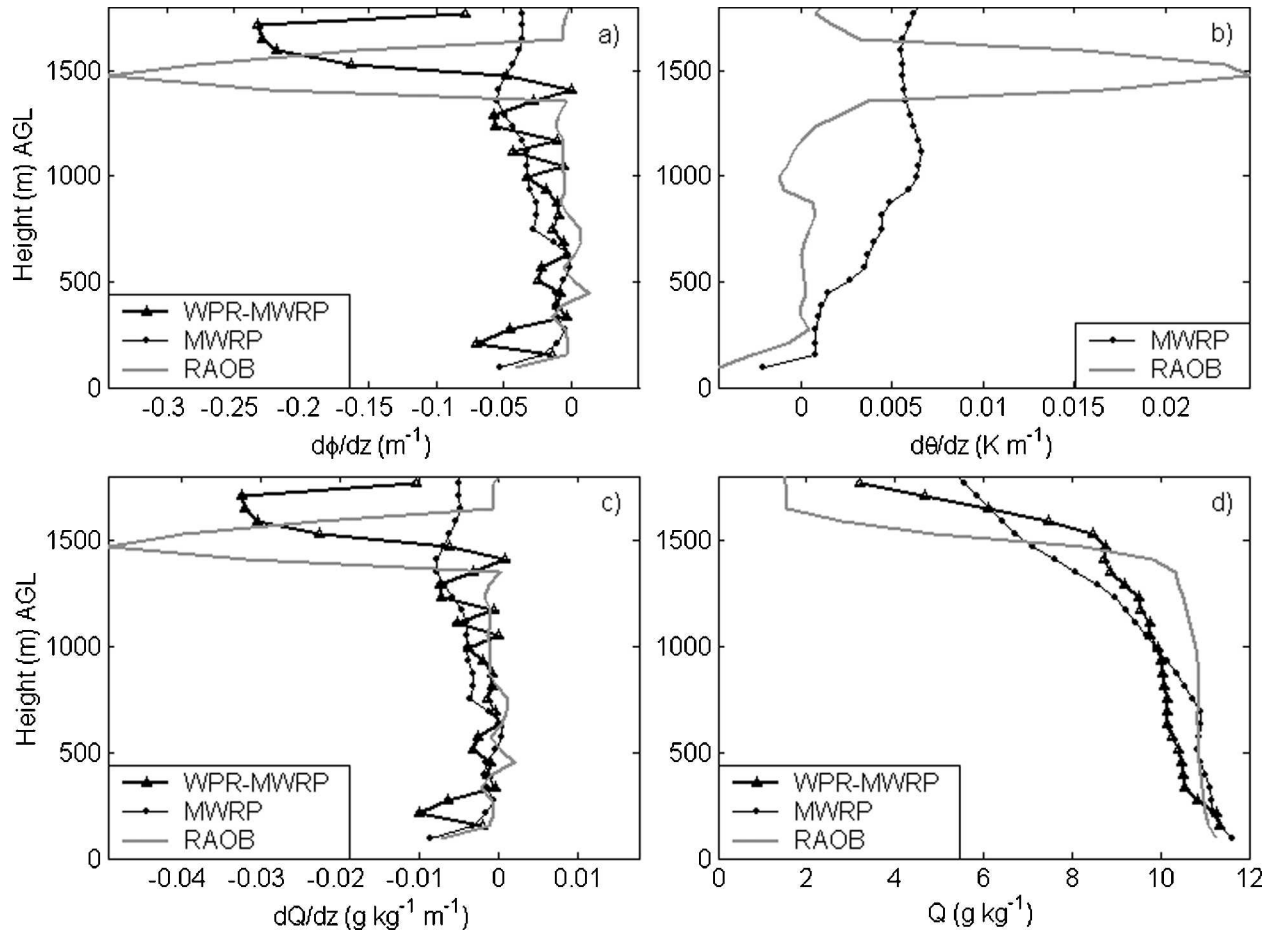
FIG. 5. As in Fig. 4, but for 2330 UTC 7 Jun 2002.

of their combination using Eq. (4) for the case of 2330 UTC 7 June 2002.

4. Case studies

In this section we analyze measurements collected during June 2002 at the ARM SGP site in order to illustrate the performance of the method on real observations. The data we were able to access were collected by a MWRP and a WPR, which have been introduced, together with the respective retrieval techniques, in section 2. Also, radiosonde balloons were launched at the same site every 6 h.

In Fig. 4 we present results relative to the case study of 2330 UTC 6 June 2002. Vertical gradients of potential refractivity ($d\phi/dz$) and of potential temperature ($d\theta/dz$) as measured by radiosonde and estimated by MWRP are presented together with vertical gradient profiles of specific humidity (dQ/dz), as measured by radiosonde, estimated by MWRP, and obtained by the combination of $d\phi/dz$ and $d\theta/dz$ as described in Eq. (4).

Raob data are reduced to significant altitudes (relative to the measurements heights of the wind profiler). The profile of $d\phi/dz$, as computed with the use of Eq. (6), had the sign ambiguity solved looking at the microwave radiometer estimates of $d\phi/dz$ profile. This approach makes the technique completely remote-sensed and independent from simultaneous in situ radiosonde measurements. As expected, the vertical resolution achieved by MWRP is much lower than the one of the radiosonde for what concerns both $d\phi/dz$ and $d\theta/dz$ profiles. Although, coupling WPR and MWRP measurements, we significantly increase the vertical resolution of $d\phi/dz$. Moreover, we point out that values of $d\theta/dz$ are about one order of magnitude smaller than values of $d\phi/dz$, and thus of second order with respect to $d\phi/dz$ in Eq. (4). Finally, in Fig. 4d are shown profiles of specific humidity, as measured by radiosonde, retrieved by MWRP and obtained by integrating dQ/dz profile retrieved by the combined technique. Note that the value of Q at the first level of the profile and its integrated value up to the maximum height reached by
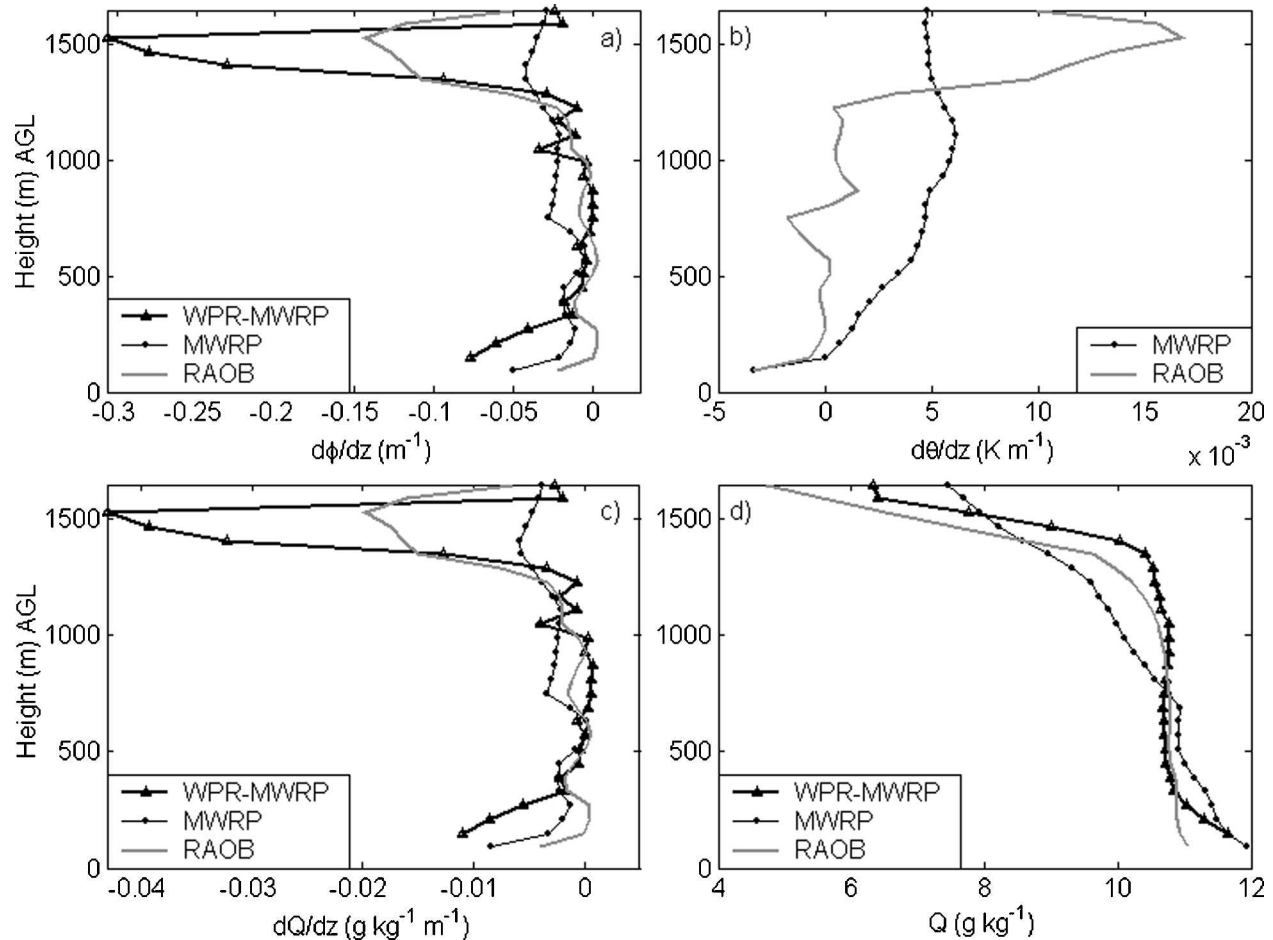
FIG. 6. As in Fig. 4, but for 2330 UTC 17 Jun 2002.

WPR measurements are constrained considering equivalent quantities estimated by MWRP, in order to make the most of the well established accuracy for integrated content retrieval by microwave radiometry. The vertical profile of Q derived with the combined technique seems to correct for the artifact shown by the MWRP estimate between 600 and 1200 m and to follow better the trend shown by the radiosounding. Hereafter altitude is given in meters above the ground level (AGL). Differences in the radiosonde and MWRP humidity sensor measurements in the first level lead to a bias that remains present along the entire vertical range. This difference might be related to random error affecting the two independent sensors, but also to the small-scale variability of the humidity field. Also, some kinds of radiosonde humidity sensors have found to be biased. For example, Turner et al. (2003) analyzed an ensemble of 6-yr ARM SGP radiosondes (1994–2000), and found differences of greater than 25% in IWV, when considering data from dual-sonde soundings. Since September 2000, the operational radiosondes de-

ployed at ARM SGP belongs to a new generation packaging, which is supposed to increase the quality of humidity measurements (Cimini et al. 2002), although a systematic analysis is still under study.

Figure 5 presents the same plots as in the previous, but for the case study of 2330 UTC 7 June 2002. Figure 5d shows that the combined technique follows better the sharp humidity drop measured by radiosonde, although there is a vertical shift of about 100 m, as also revealed by the vertical profiles of dQ/dz. However, as shown by Bianco et al. (2003), the height of the peak in the WPR-MWRP dQ/dz profile is consistent with the fact that the refractive index structure parameter (C_n^2) presents a local maximum at the entrainment zone at some 1650 m for the same hour. Thus, the vertical shift between the two measurements might be related to horizontal drift of the balloon rather than to a displacement of the combined technique estimate.

Figure 6 presents the same analysis, but for the case study of 2330 UTC 17 June 2002. Also in this case the results obtained with the combined technique show an
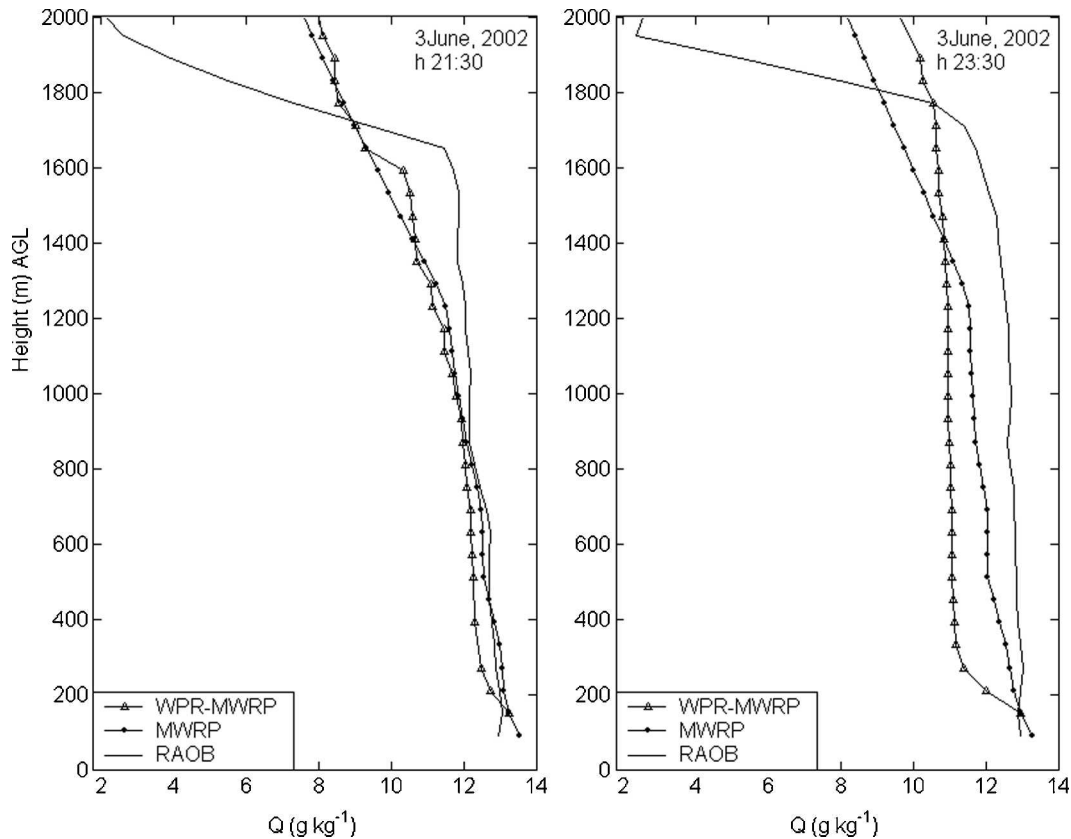
FIG. 7. Retrieved humidity vertical profiles (Q) obtained from the integration of dQ/dz as measured by radiosonde (solid gray line), estimated by MWRP (dotted line), and computed with the combined technique (solid black line with triangles at measurement heights).

enhanced vertical structure compared to the original MWRP retrieval, following in greater detail the radiosonde observation. Indeed, the sharp humidity drop at 1400 m is well detected both in intensity and vertical position. However, we note that the vertical profile of Q estimated by the combined technique presents a sharp gradient below 300 m, which does not exhibit either in radiosonde or in MWRP observations. We believe this is related to a peak in the vertical squared gradient of the horizontal wind $[(dV_h/dz)^2]$ revealed at the same height, as we demonstrate below.

Figure 7 presents two examples (2130 UTC 3 June 2002; 2330 UTC 3 June 2002) in which the combined algorithm seems to not outperform the MWRP in retrieving the vertical humidity profile, when we compare with radiosonde observations. In the first case, our method does not bring any improvement with respect to the MWRP retrieval. In the second case, it is evident how the combined technique identifies a strong gradient below 300 m, which is not present in the radiosounding. In both cases the remote observations estimates clearly miss the sharp and well-defined humidity

gradients centered around 1700–1800 m detected by in situ measurements.

It is worth mentioning that spatial and temporal differences in the radiosonde and radiometer measurements can be significant, particularly during convective or broken cloud conditions. During the ascension, the radiosonde is subject to wind drifting and usually departs from the vertical direction. In this perspective, the radiosonde may measure particular conditions in a volume that is not in the field of view of the MWRP and WPR. However, for the two cases in Fig. 7, no cloud or strong convective conditions were observed, as depicted by the time–height cross sections of radiometric retrievals shown in Fig. 8. Thus, we believe that the disagreement between in situ and remote estimates in Fig. 7 is not mainly related to radiosonde wind drifting.

To track down the reasons for this disagreement, we investigate in greater detail the various contributions to the computation of dQ/dz.

Hourly radar-obtained vertical profiles for C_ϕ^2, C_w^2, and $(dV_h/dz)^2$, as measured by the WPR, are presented in Fig. 9. Note that the vertical profile of $(dV_h/dz)^2$ is
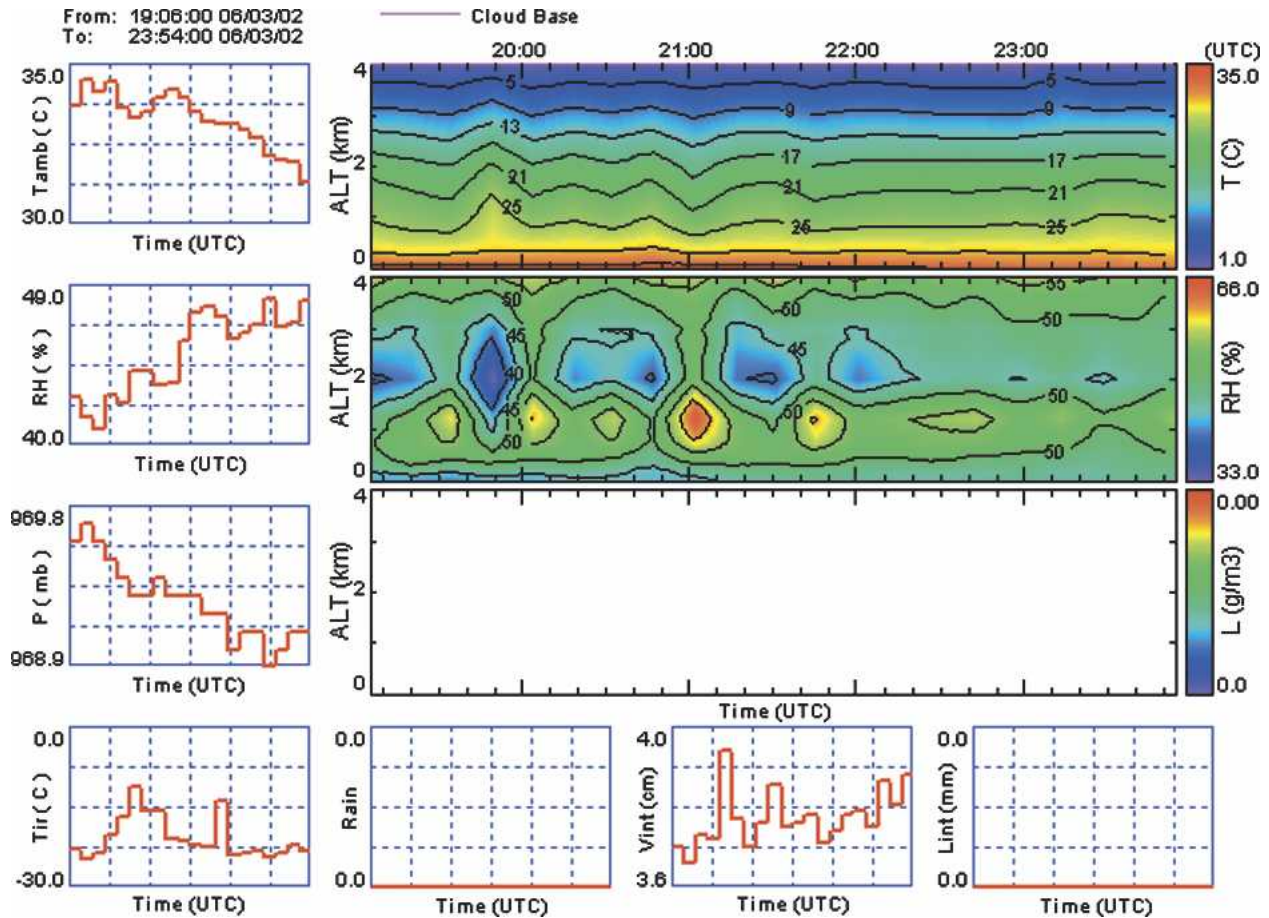
FIG. 8. Time series of temperature, relative humidity, and pressue at (left) ground level; (bottom) infrared temperature, rain flag, integrated vapor, and integrated liquid; and time–height cross sections of MWRP profile retrievals for 3 Jun 2002.

obtained directly from the radar-derived consensus files and thus no postprocessing procedures are applied. In Fig. 9c we also plot the vertical profile of $(dV_H/dz)^2$ as measured by radiosonde. The lack of data in the vertical profiles (Figs. 9c–e) between 400 and 500 m is due to the consensus algorithm screening, which did not find enough valid measurements for the radial velocities over the considered period. Large differences are evident below 400 m where the WPR detects a strong gradient that is not present in the radiosounding. On the other hand, the same profile shows several relatively strong peaks between 900 and 1400 m. By solving Eq. (6) with the two profiles of $(dV_H/dz)^2$, we obtain different values of $d\phi/dz$, as illustrated in Fig. 9d. In the case of using $(dV_H/dz)^2$ from the consensus file we note a sharp gradient near the surface, which is not revealed when using the $(dV_H/dz)^2$ profile as measured by radiosonde. The opposite happens around 1900-m height where the dotted line seems to reproduce the sharp peak of C_ϕ^2. In the same figure are shown vertical profiles of dQ/dz as obtained from Eq. (4) via $d\phi/dz$ pro-

files, and as computed from radiosonde observations. Comparing Figs. 9d and 9e it is evident how dQ/dz, obtained from Eq. (4), preserves the same structural features of $d\phi/dz$. Finally, vertical specific humidity profiles are also presented.

The poor performances in the combined technique could be attributable to the strong and rather inaccurate peculiarities of $(dV_H/dz)^2$ as obtained from WPR consensus files. Indeed, substituting in situ measurements of $(dV_H/dz)^2$ in Eq. (6), we can correct inadequacies both at low and high altitudes.

As another example in Fig. 10 we show the case of 2130 UTC 3 June 2002. The radar detects again a strong gradient of V_h below 400 m. This feature is not present in the radiosonde sounding. Differences in these two profiles impact the humidity profile retrieval (Fig. 10f). The bias between the in situ and remotely sensed profiles increases with height because of the features just mentioned. On the other hand, using $(dV_H/dz)^2$ derived from the radiosonde definitely improves the estimate of Q when compared with in situ measurements.
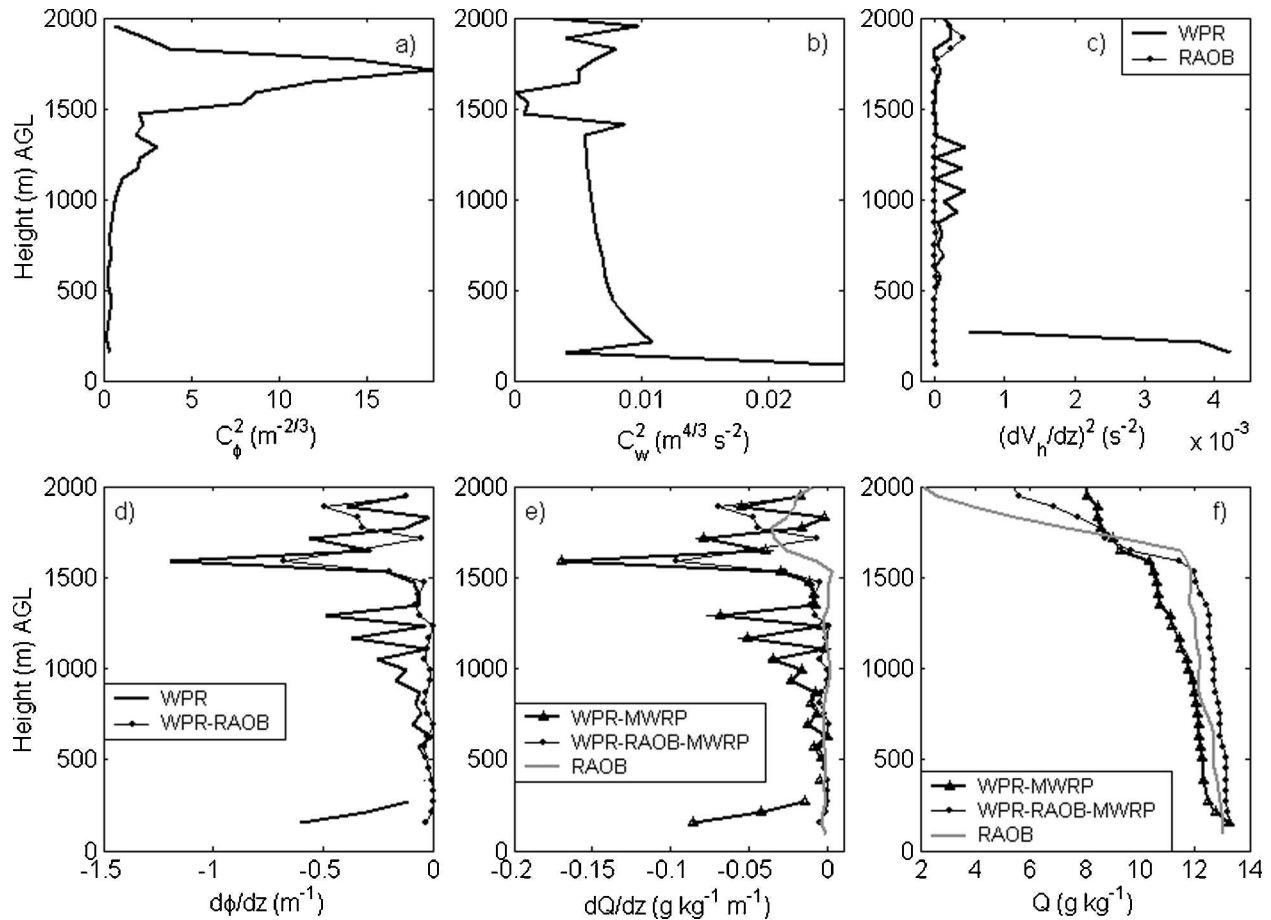
FIG. 9. 2330 UTC 3 Jun 2002: (top) hourly radar-obtained vertical profiles for (a) C_ϕ^2; (b) C_w^2; (c) $(dV_H/dz)^2$ (solid line is the one obtained from the radar-derived consensus files, dotted line is relative to raob measurements); (bottom) (d) $d\phi/dz$ obtained combining in Eq. (6) C_ϕ^2, C_w^2, and $(dV_H/dz)^2$ [solid line is retrieved using $(dV_H/dz)^2$ from consensus files and dotted line using $(dV_H/dz)^2$ from radisonde]; (e) retrieved humidity gradient profiles (dQ/dz) obtained from the combination of the previous variables with the use of Eq. (4) in which for the solid line, with triangles at measurement heights, $(dV_H/dz)^2$ is the radar-derived one, for the dotted line $(dV_H/dz)^2$ is the raob-measured one, and the solid thin line represents dQ/dz measured by radiosonde; and (f) vertical humidity profiles (Q) obtained from the integration of the various dQ/dz.

A possible way to tackle some deficiencies of the combined technique, as illustrated before, could be to generate the consensus file directly from the raw spectral moment data, as computed on the postprocessed spectra via the fuzzy logic approach. In this perspective all the cases have been reanalyzed using, in Eq. (6), $(dV_H/dz)^2$ recomputed from the moments obtained by the postprocessing procedure. Figure 11 shows a summary of the results for each case study and a comparison between the different methods. Vertical humidity profiles are obtained for 1 June (2330), 3 June (2130), 3 June (2330), 6 June (2330), 7 June (2330), and 17 June (2330). The line representing vertical humidity profiles retrieved using in Eq. (6) radar-derived $(dV_H/dz)^2$ from original consensus files is denoted by "WPR-MWRP"; the one representing vertical humidity profiles re-

trieved using in Eq. (6) postprocessed radar-derived $(dV_H/dz)^2$ from recomputed consensus files is denoted by "WPR FL-MWRP"; the line relative to Q retrieved from MWRP observations is denoted by "MWRP"; finally, the line representing Q as measured by radiosonde is denoted by "RAOB". Profiles relative to cases 3 June (2130), 3 June (2330), and 17 June (2330) seem to follow more closely radiosonde data even if for the cases study 1 June (2330), 6 June (2330), and 7 June (2330) such improvement is no apparent.

Although the scope of this work was essentially to introduce the potential of this physical self-consistent remote sensing technique, a first statistical analysis of the results is presented in Table 1. However, we stress the fact that these statistics do not represent a definite validation due to the limited number of considered case studies.
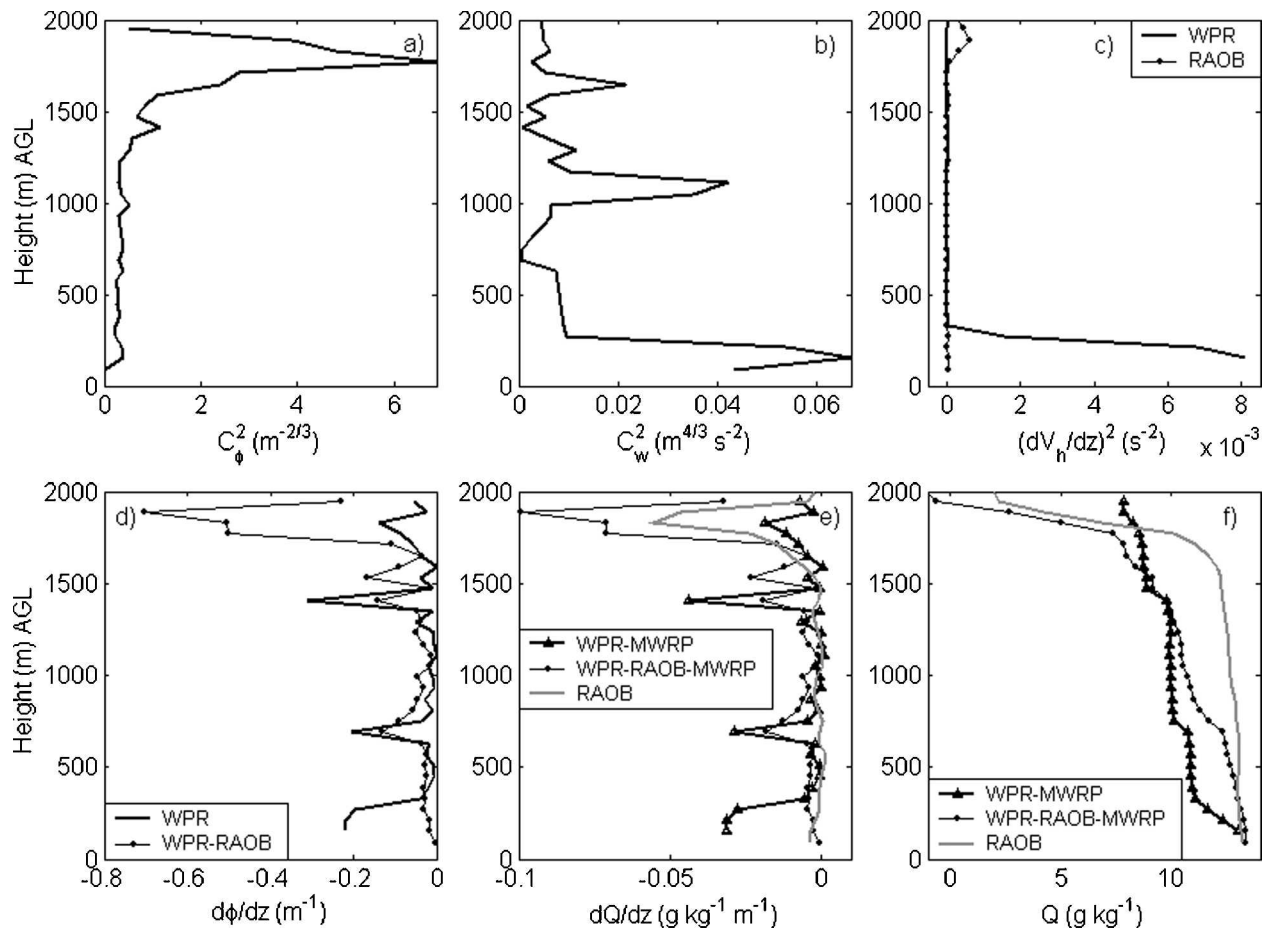
FIG. 10. As in Fig. 9, but for 2130 UTC 3 Jun 2002.

The statistics compare vertical humidity profiles as measured by radiosonde and remote sensing techniques. We show results for humidity profiles obtained using MWRP only, MWRP and WPR with $(dV_H/dz)^2$ obtained from the original consensus radar data (WPR-MWRP), and MWRP and WPR with $(dV_H/dz)^2$ obtained from postprocessed radar data (WPR FL-MWRP). The statistics are relative to the entire set of the analyzed cases and they include correlation coefficients of radiosonde and remote sensing humidity profiles, and mean values; standard deviation, and root-mean-square of the differences of the two.

The value of the mean difference given by WPR FL-MWRP confirms that this method is in mean as accurate as the MWRP. On the other hand the proposed method improves by a 10% both the value of the standard deviation and of rms with respect to microwave passive techniques. Moreover, the WPR FL-MWRP shows a slightly improved correlation compared to microwave radiometer alone.

Overall, the proposed method, with the fuzzy logic postprocessed consensus files, outperforms both the passive technique and the combined method that makes use of the original consensus radar files, but an extensive validation on a larger dataset is opportune in order to quantitatively estimate the improvements brought by the proposed technique.

5. Summary and conclusions

In this paper we presented a technique for improving resolution and accuracy of atmospheric humidity profiling based on the combination of passive and active remotely sensed measurements. This self-consistent remote sensing physical method relies on the relationship between the gradients of the specific humidity, potential refractivity, and potential temperature as described by Eq. (5) (Stankov et al. 2003). The described approach has the advantage that it is independent from in situ measurements, although we compare with radiosoundings for validation purposes. In fact, we derive the potential refractivity gradient from wind profiler ra-
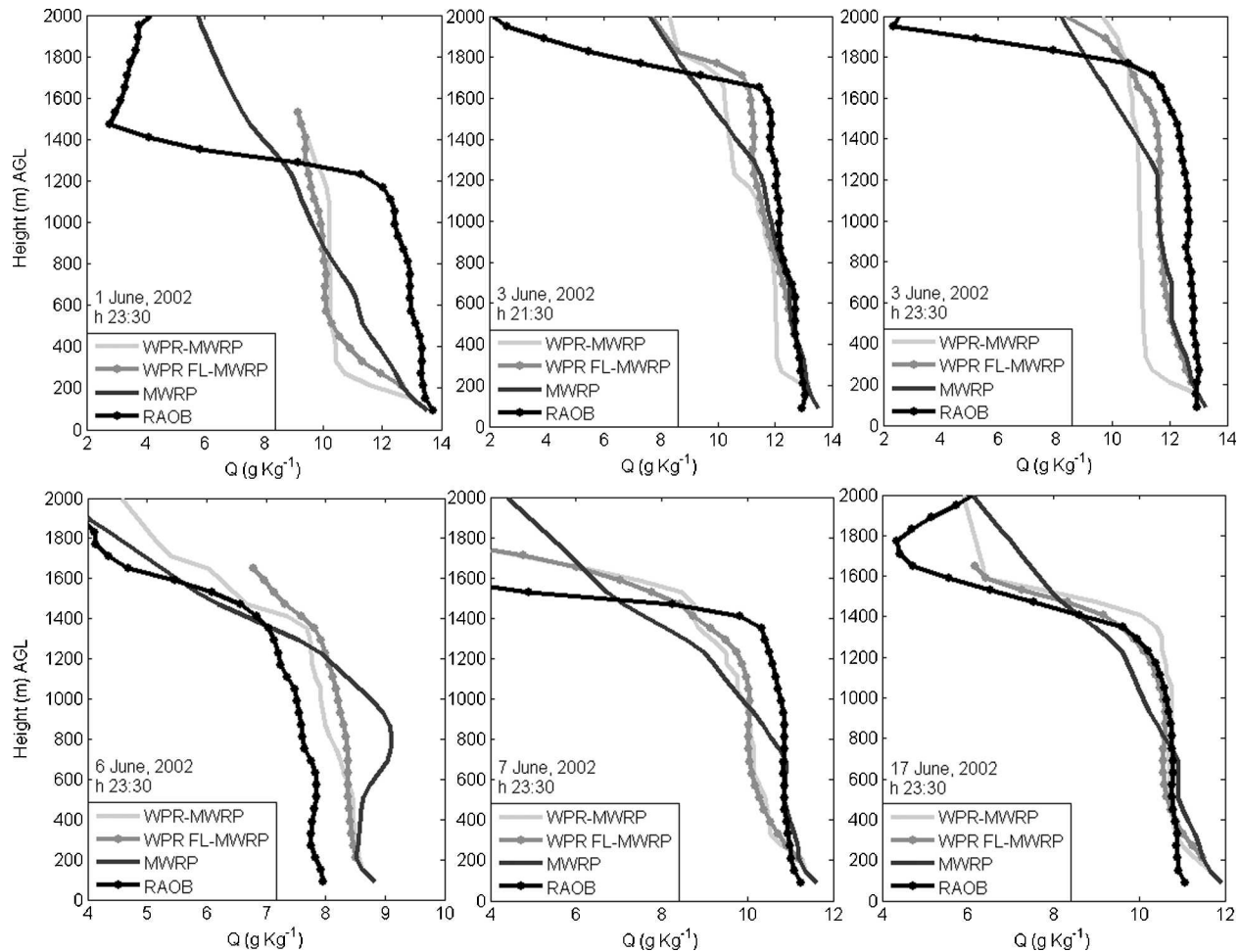
FIG. 11. Vertical humidity profiles (Q) obtained for the cases under analysis. For the WPR-MWRP lines, $(dV_h/dz)^2$ of Eq. (6) is the radar-derived one; for the WRP FL-MWRP lines, $(dV_h/dz)^2$ is the postprocessed radar-derived one; darker gray lines are relative to Q retrieved from MWRP observations only; black lines represent Q as measured by radiosonde.

dar (WPR) data, while potential temperature gradient is estimated from multichannel microwave radiometer profiler (MWRP) observations.

The empirical set of data was collected during June 2002 at the Atmospheric Radiation Measurement (ARM) Program's Southern Great Plains (SGP) site in Oklahoma from a 915-MHz wind profiler and a MWRP. We postprocessed the raw measurements from the two instruments using recent developments in data analysis including fuzzy logic (Bianco and Wilczak 2002) and neural networks (Solheim et al. 1998).

We focused our attention on some case studies, although an extensive analysis, concerning the whole dataset, is in preparation. Particularly, for cases during 6, 7, and 17 June (Figs. 4, 5, and 6), we showed that the combined technique is able to capture sharp gradients in the humidity profiles, enhancing the vertical resolution of the MWRP estimates, as demonstrated by the

comparison with simultaneous radiosoundings. Moreover, the humidity profiles retrieved with the combined technique keep the well-known accuracy of microwave radiometry for integrated water vapor content, as we used this information as a constraint. The use of WPR by itself, or in combination with a Radio Acoustic Sounding System (RASS) for potential temperature estimates, would not guarantee this advantage. Even adding a GPS receiver, it would provide the total, not the partial, integrated water content. However, an array of GPS receivers could provide humidity vertical structure by tomography, as discussed by MacDonald et al. (2002).

The proposed technique has the limit to work well during convective periods, when the turbulence is well developed. This explains why case studies analyzed in this work happened all around 2200 UTC. However, even limiting our sample to these hours, we experi-

TABLE 1. Statistical comparison of the analyzed retrieval methods in terms of: mean error (g kg^{-1}), std dev (g kg^{-1}), rms (g kg^{-1}), correlation coefficient, and number of available points. The statistics compares vertical humidity values as measured by radiosonde vs vertical humidity values obtained from 1) MWRP, 2) the combined technique where $(dV_H/dz)^2$ was derived from the original consensus radar data (WPR-MWRP), and 3) the combined technique where $(dV_H/dz)^2$ was derived from postprocessed radar data (WPR FL-MWRP).

Method	Mean	Std dev	Rms	Corr. coef.	No. pts.
MWRP	0.14	1.53	1.54	0.88	154
WPR-MWRP	0.37	1.44	1.49	0.89	154
WPR FL-MWRP	0.13	1.38	1.39	0.91	154

enced several unsatisfactory cases in which the combined technique did not outperform MWRP estimates, as reported in Fig. 7. In a deeper analysis (Figs. 9 and 10) we found out that the use of vertical gradients of the horizontal wind as computed by standard consensus algorithms strongly influences the quality of the humidity profile retrieval. For this reason we decided to use reprocessed consensus files derived from moments data, as computed on the postprocessed spectra. In this perspective all the cases have been reanalyzed comparing different methods and a statistical analysis on the case study has been performed.

Possible improvements of the proposed technique concern both data processing and experimental setup. On the first side, we could use a statistical, rather than analytical, approach to derive the humidity profile from the remote observations (Stankov 1998). Although other investigators (Gossard et al. 1999) found a good agreement comparing the two methods, the statistical approach provides tools for making the estimate possibly more robust. On the other hand, we have to consider that the present experimental setup was not designed for this purpose, and much shrewdness could be adopted for the purpose. As pointed out by Stankov et al. (2003), the more powerful 449-MHz radar system performs better than the 915 MHz one, due to its narrower beam. Also, by increasing the number of points in the spectral domain of the WPR acquisition, we would obtain a better resolution on the vertical radial velocity computation, which could improve the retrieval of the structure parameter of vertical velocity. Further improvements might come from the optimization of other settings, such as the dwell time. Moreover, ground-based MWRP estimates of temperature and humidity profiles could be further improved by coupling these measurements with those available from other sensors, such as satellite radiometers and ground-based Raman lidars.

In summary, we presented a technique, developed first by Gossard et al. (1982) and then by Stankov et al. (1996, 2003), for the retrieval of specific humidity profiles, and we adapted it in order to rely only on remote observations, thus being completely independent from in situ measurements. We illustrate the performance of the method on real observations by comparing with simultaneous radiosoundings. We showed how the active–passive combined approach can increase the vertical resolution by capturing sharp gradients in the humidity profile without degrading the original accuracy for passive integrated content retrieval. We also presented two cases in which the combined technique was unsatisfactory, and we gave a hint for likely causes. The proposed method outperforms the technique based on passive observations, but an extensive validation on a larger dataset must be performed in order to quantitatively estimate the improvements brought by the proposed technique.

Finally, we discussed possible improvements both in the data processing and in the experimental setup, which might be considered in our future research.

REFERENCES

Bianco, L., and J. M. Wilczak, 2002: Convective boundary layer mixing depth: Improved measurement by Doppler radar wind profiler using fuzzy logic. *J. Atmos. Oceanic Technol.,* **19,** 1745–1758.

——, D. Cimini, R. Ware, and F. S. Marzano, 2003: Combining microwave radiometer and wind profiler radar measurements to improve accuracy and resolution of atmospheric humidity profiling. *Proc. Int. Geosci. Remote Sens. Symp. (IG-ARSS03)*, Toulouse, France, IEEE.

Cimini, D., E. R. Westwater, and B. Lesht, 2002: Evaluation of the improvements in humidity sounding by balloon-borne sensors. *Proc. of the COST720 Meeting*, L'Aquila, Italy, COST. [Available online at http://www.cost720.rl.ac.uk/].

——, ——, Y. Han, and S. J. Keihm, 2003: Accuracy of ground-based microwave radiometer and balloon-borne measurements during the WVIOP2000 field experiment. *IEEE Trans. Geosci. Remote Sens.,* **41,** 2605–2615.

Cohn, S. A., 1995: Radar measurements of turbulent eddy dissipation rate in the troposphere: A comparison of techniques. *J. Atmos. Oceanic Technol.,* **12,** 85–95.

Cornman, L. B., R. K. Goodrich, C. S. Morse, and W. L. Ecklund, 1998: A fuzzy logic method for improved moment estimation

from Doppler spectra. *J. Atmos. Oceanic Technol.,* **15,** 1287–1305.

Furumoto, J., M. Kurimoto, and T. Tsuda, 2003: Continuous observations of humidity profiles with the MU radar-RASS combined with GPS and radiosonde measurements. *J. Atmos. Oceanic Technol.,* **1,** 23–41.

Gossard, E. E., 1990: Radar research on the atmospheric boundary layer. *Radar in Meteorology,* D. Atlas, Ed., Amer. Meteor. Soc., 477–527.

——, R. R. Chadwick, W. D. Neff, and K. P. Moran, 1982: The use of ground based Doppler radars to measure gradients, fluxes and structure parameters in elevated layers. *J. Appl. Meteor.,* **21,** 211–226.

——, D. C. Welsh, and R. G. Strauch, 1990: Radar-measured height profiles of C_n^2 and turbulence dissipation rate compared with radiosonde data during October 1989 at Denver. NOAA Tech. Rep. ERL 442-WPL 63, Enviromental Research Laboratories, 115 pp. [Available from NOAA/ERL/ETL Broadway, Boulder, Co, 80305.]

——, R. G. Strauch, B. B. Stankov, and D. E. Wolfe, 1995: Measurements of property gradients and turbulence aloft with ground-based Doppler radars. NOAA TM ERL 453-ETL 67, Enviromental Technology Laboratory, 31 pp. [Available from the National Technical Information Service, 5285 Port Royal Rd., Springfield, VA, 22161.]

——, D. E. Wolfe, K. E. Moran, R. A. Paulus, D. K. Anderson, and L. T. Rogers, 1998: Measurements of clear-air gradients and turbulence properties with radar wind profilers. *J. Atmos. Oceanic Technol.,* **15,** 321–342.

——, S. Gutman, B. B. Stankov, and D. E. Wolf, 1999: Profiles of radiorefractive index and humidity derive from radar wind profilers and the Global Position System. *Radio Sci.,* **34,** 371–383.

Güldner, J., and D. Spänkuch, 2001: Remote sensing of the thermodynamic state of the atmospheric boundary layer by ground-based microwave radiometry. *J. Atmos. Oceanic Technol.,* **18,** 925–933.

Han, Y., and E. R. Westwater, 2000: Analysis and improvement of tipping calibration for ground-based microwave radiometers. *IEEE Trans. Geosci. Remote Sens.,* **38,** 1260–1276.

Jordan, J. R., R. J. Lataitis, and D. A. Carter, 1997: Removing ground clutter and intermittent clutter contamination from wind profiler signal using wavelet transforms. *J. Atmos. Oceanic Technol.,* **14,** 1280–1297.

Liljegren, J., 2004: Improved retrievals of temperature and water vapor profiles with a twelve-channel radiometer. *Proc. Eighth Symp. on Integrated Observing and Assimilation Systems for Atmosphere, Oceans and Land Surface*, Seattle, WA, Amer. Meteor. Soc., 4.7.

MacDonald, A., Y. Xie, and R. Ware, 2002: Diagnosis of three-dimensional water vapor using slant observations from a GPS network. *Mon. Wea. Rev.,* **130,** 386–397.

May, P. T., and R. G. Strauch, 1989: An examination of wind profiler signal processing algorithms. *J. Atmos. Oceanic Technol.,* **6,** 731–735.

Schroeder, J., and E. R. Westwater, 1991: User's guide to microwave radiative transfer software. NOAA Tech. Memo. ERL WPL-213, 84 pp.

Solheim, F., and J. R. Godwin, 1998: Passive ground-based remote sensing of atmospheric temperature, water vapor, and cloud liquid water profiles by a frequency synthesized microwave radiometer. *Meteor. Zeitschrift,* **7,** 370–376.

——, ——, E. Westwater, Y. Han, S. Keihm, K. Marsh, and R. Ware, 1998: Radiometric profiling of temperature, water vapor, and liquid water using various inversion methods. *Radio Sci.,* **33,** 393–404.

Stankov, B. B., 1998: Multisensor retrieval of atmospheric properties. *Bull. Amer. Meteor. Soc.,* **79,** 1835–1854.

——, E. R. Westwater, and E. E. Gossard, 1996: Use of wind profiler estimates of significant moisture gradients to improve humidity profile retrivial. *J. Atmos. Oceanic Technol.,* **13,** 1285–1290.

——, E. E. Gossard, B. L. Weber, R. J. Lataitis, A. B. White, D. E. Wolfe, and D. C. Welsh, 2003: Humidity gradient profiles from wind profiling radars using the NOAA/ETL advanced Signal Processing System (SPS). *J. Atmos. Oceanic Technol.,* **20,** 3–22.

Strauch, R. G., D. A. Merritt, K. P. Moran, K. B. Earnshaw, and D. van de Kamp, 1984: The Colorado wind profiling network. *J. Atmos. Oceanic Technol.,* **1,** 37–49.

Turner, D., B. Lesht, A. Clough, J. Liljegren, H. Revercomb, and D. Tobin, 2003: Dry Bias and Variability in Vaisala RS80-H Radiosondes: The ARM Experience. *J. Atmos. Oceanic Technol.,* **20,** 117–132.

Ware, R., F. Solheim, R. Carpenter, J. Gueldner, J. Liljegren, T. Nehrkorn, and F. Vandenberghe, 2003: A multi-channel radiometric profiler of temperature, humidity and cloud liquid. *Radio Sci.,* **38,** 8079, doi:10.1029/2002RS002856.

Weber, B., D. Welsh, D. Merrit, D. Wuertz, D. Wolfe, and T. Wilfong, 2004: A new paradigm for Doppler radar wind profiler signal processing. NOAA Tech. Memo OAR ETL-306, 233 pp.

Westwater, E. R., 1993: Ground-based microwave remote sensing of meteorological variables. *Atmospheric Remote Sensing by Microwave Radiometry*, M. A. Janssen Ed., Wiley, 145–213.

——, B. B. Stankov, D. Cimini, Y. Han, J. A. Shaw, B. M. Lesht, and C. Long, 2003: Radiosonde humidity soundings and microwave radiometers during NAURU99. *J. Atmos. Oceanic Technol.,* **20,** 953–971.

White, A. B., R. J. Lataitis, and R. S. Lawrence, 1999: Space and time filtering of remotely sensed velocity turbulence. *J. Atmos. Oceanic Technol.,* **16,** 1967–1971.

Wilczak, J. M., and Coauthors, 1995: Contamination of wind profiler data by migrating birds: Characteristics of corrupted data and potential solutions. *J. Atmos. Oceanic Technol.,* **12,** 449–467.